

Oxidation Chemistry of 3,7-Dimethylxanthine – a Central Behavioural Stimulant at Solid Electrodes

Rajendra N. Goyal and Arshi Rastogi*

Department of Chemistry, University of Roorkee, Roorkee – 247 667, India

Received February 15, 1999; revised December 3, 1999; accepted December 3, 1999

The electrochemical oxidation of 3,7-dimethylxanthine has been studied in the pH range 2.1–10.7 at pyrolytic graphite, platinum and glassy carbon electrodes. The electrooxidation of 3,7-dimethylxanthine at solid electrodes proceeds in a single $4e$, $4H^+$ pH dependent step to give a diimine species which decomposes in chemical followup steps. The UV absorbing intermediate generated during electrooxidation of 3,7-dimethylxanthine decayed approximately at the same rate as that of xanthine and followed the first order kinetics. The products of electrooxidation of 3,7-dimethylxanthine were characterized and a reaction scheme is suggested to explain their formation. The effect of introducing methyl groups into the electrooxidation of xanthine is also presented.

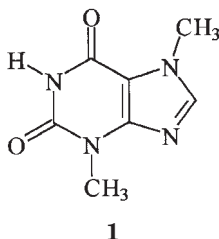
Key words: electrochemical oxidation, 3,7-dimethylxanthine

INTRODUCTION

Methylated xanthines possess a remarkable potency as adenosine antagonists¹ and inhibit many of its physiological effects. The central behavioural stimulant activity of theobromine and other methylated xanthines was shown to be correlated with their potencies by Snyder *et al.*² Xanthines also have cardiovascular effects in man³ and play an important role in the management of asthma.⁴ 3,7-Dimethylxanthine has been found to partially override the mitotic block induced by ionizing radiation in the human bladder carcinoma cell line RT 112.⁵ In view of the importance of methylxanthines as drugs, it was considered desirable to study the electrooxidation of a sim-

* Author to whom correspondence should be addressed.

ple dialkyl xanthine, 3,7-dimethylxanthine (**1**) at a stationary pyrolytic graphite electrode, glassy carbon electrode and platinum electrodes. It was observed that the electrode reaction at pyrolytic graphite and the glassy carbon electrode was essentially similar whereas no oxidation peak was observed at the platinum electrode.



EXPERIMENTAL

3,7-Dimethylxanthine (Research Biochemical Inc. MA, USA) and 3,7-dimethyluric acid (Adams Chemical Co. USA) were used as received. *N,N*-bis(trimethylsilyl) trifluoroacetamide (BSTFA) and silylation grade acetonitrile were obtained from Pierce Chemical Co., USA. Electrochemical studies were performed in Phosphate buffers⁶ of ionic strength of 0.5 M, prepared from reagent grade chemicals. All potentials are referred to the SCE at an ambient temperature of 20 ± 2 °C.

Voltammetric studies were carried out on a Cypress Model CS-1090 microprocessor based electrochemical system and spectral studies during electrolysis were carried out on a Beckman DU-6 spectrophotometer. The working electrodes (pyrolytic graphite, glassy carbon and platinum) were prepared by the method reported earlier⁷ and had an area of 8, 12 and 3 mm², respectively. The surfaces of the PGE and platinum electrodes were renewed each time by polishing on a 600 grit metallographic polishing disc while that of GCE was renewed by the procedure of Chan *et al.*⁸

The stock solution of 3,7-dimethylxanthine (1 mM) was prepared in doubly distilled water. For voltammetric studies, 2 mL of stock solution was mixed with 2 mL of phosphate buffer of appropriate pH and the nitrogen gas was bubbled for 8–10 min before recording the voltammograms. Controlled potential electrolysis of 3,7-dimethylxanthine was carried out at different pH in a conventional H-type cell using a rectangular pyrolytic graphite plate (6×1 cm²) or glassy carbon rod (6×0.5 cm²) as working, cylindrical platinum gauze as auxiliary and SCE as reference electrode, respectively. The number of electrons involved in electrooxidation was determined by graphical integration of the current time curve as reported by Lingane.⁹

For products separation, 8–10 mg of 3,7-dimethylxanthine was electrooxidized by applying a 100 mV more positive potential to the anodic peak I_a . The progress of electrooxidation was monitored by observing the decrease in peak current I_a in cyclic voltammetry. When peak I_a completely disappeared, the exhaustively electrolyzed solution was removed from the cell and lyophilized. The freeze-dried material was dissolved in 1–2 mL of water and passed through a glass column packed with Sephadex G-10, using doubly distilled water as eluent. The flow-rate was adjusted to 1.0 mL/min. Fractions (5 mL each) were collected and their absorbance was moni-

tored at 210 nm. The absorbance was then plotted against the volume. At pH 3.0, three peaks – P₁ (150–190 mL), P₂ (190–200 mL) and P₃ (225–275 mL) were observed whereas at pH 7.0 only two peaks – P₁ (150–200 mL) and P₄ (220–250 mL) were noticed. The volume under these peaks separately collected and lyophilized. The dried material obtained was analyzed by m.p., ¹H NMR and mass spectra.

IR spectra of the products were recorded as KBr pellets using a Perkin-Elmer FTIR spectrometer. Mass spectra were recorded on a Jeol, JMS D 300 instrument. For silylation, about 500–100 µg of the product was treated with BSTFA – acetonitrile (50 µL each) in a sealed 3.0 mL vial at 110 °C for 10–15 min in an oil bath. The vial was then cooled at room temperature and 2 µL of the sample was injected into the GC-MS.

RESULTS AND DISCUSSION

Linear sweep voltammetry of 0.5 mM 3,7-dimethylxanthine at a sweep rate of 10 mV s⁻¹ exhibited a single well-defined anodic peak (I_a) only in the pH range 7.0–10.7 at PGE and GCE. No peak was observed at the platinum electrode. At pH < 7.0, the peak merged with the background and only a small clink was occasionally noticed. The peak at the GCE was much broader in comparison to PGE and the shape of peak I_a was spiky at pH > 7.0 at PGE. It was interesting to observe that peak potentials of peak I_a were more or less the same at the glassy carbon electrode and at the PGE in the entire pH range. The peak potential of peak I_a was dependent on pH and shifted to less positive values with an increase in pH in the entire pH range at both electrodes (Figure 1). The dependence of the E_p of peak I_a on pH at PGE and GCE was linear and can be described by the equation:

$$E_p \text{ (pH 7.0 – 10.7)} = [1700 - 60 \text{ pH}] \text{ mV } vs. \text{ SCE.}$$

In cyclic sweep voltammetry, at a sweep rate of 200 mV s⁻¹, a well-defined anodic peak I_a was observed only at pH > 7.0. At pH < 7.0, peak I_a was occasionally seen as a bump and, due to its high oxidation potential, it appeared to merge with the background. In the reverse sweep, a cathodic peak III_c was observed and in the subsequent sweep towards positive potentials one more anodic peak (II_a) was noticed in the pH range 2.1–6.0. Some typical cyclic voltammograms of 3,7-dimethylxanthine are presented in Figure 2. The peak potential of peak II_a was also dependent on pH and shifted to less positive potential with an increase in pH in the pH range 2.1–6.0. The plot of E_p vs. pH for peak II_a was also linear as shown in Figure 1 and can be described by the equation:

$$E_p \text{ (pH 2.1 – 6.0)} = [850 - 58 \text{ pH}] \text{ mV } vs. \text{ SCE.}$$

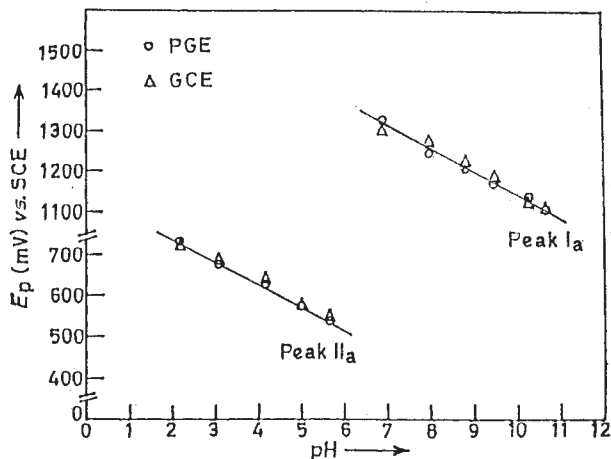


Figure 1. Dependence of E_p on pH observed for 0.5 mM 3,7-dimethylxanthine in phosphate buffers of different pH ($\mu = 0.5$ M), sweep rate 100 mV s^{-1} at PGE (O) and GCE (Δ).

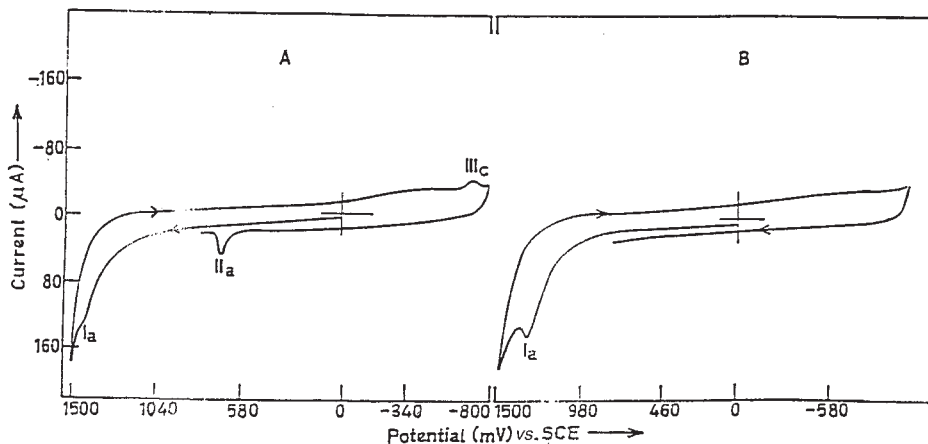


Figure 2. Typical cyclic voltammograms of 0.5 mM 3,7-dimethylxanthine at GCE (A) pH 3.0 (B) pH 7.0, sweep rate 200 mV s^{-1} .

Cyclic voltammograms were also recorded by changing the direction of the negative going sweep at different potentials. It was observed that peak II_a systematically increased when the sweep was extended to more negative potentials. This behaviour suggests that the species responsible for peak II_a

(3,7-dimethyluric acid) is formed not by oxidation of starting compound but by reduction of the 4e product at negative potentials. The presence of methyl groups in 3,7-dimethylxanthine would make *N*-3 and *N*-7 positions sufficiently electron rich due to the electron donating effect of methyl groups and hence these positions would be protonated with $pK_a > 11.0$.¹⁰

The effect of concentration on the peak current of peak I_a was studied at pH 7.0 in the concentration range 0.1 to 2.0 mM at PGE and GCE. The peak current of peak I_a increased at both electrodes with the increase in concentration of 3,7-dimethyl xanthine. The i_p versus concentration plot (Figure 3) was practically linear up to 0.4 mM concentration and had a tendency to

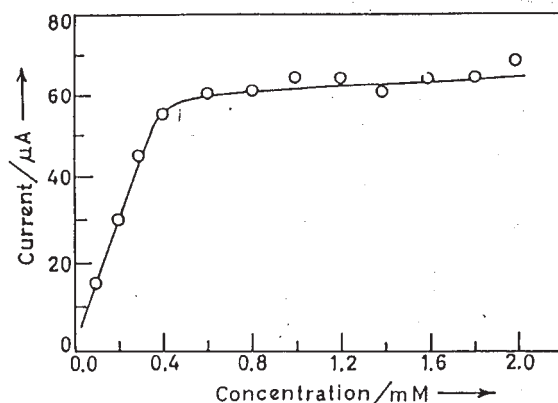


Figure 3. Dependence of peak current on concentration for 3,7-dimethylxanthine at pH 7.0, sweep rate 100 mV s^{-1} .

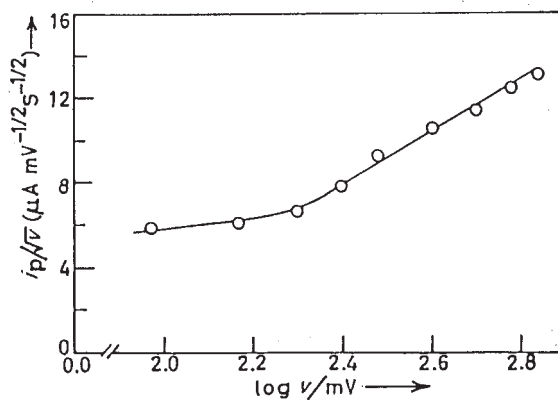


Figure 4. Plot of i_p/\sqrt{v} vs. logarithm of sweep rate for peak I_a of 0.5 mM 3,7-dimethylxanthine at pH 7.0.

limit at higher concentrations. This behaviour suggested adsorption of 3,7-dimethylxanthine at the surface of GCE and PGE.¹¹ The adsorption complications¹² were further confirmed by the increase in peak current function (i_p/\sqrt{v}) with the increase in $\log v$ (Figure 4).

The effect of sweep rate on the E_p of peak I_a was studied in the sweep range of 50–800 mV s^{-1} at PGE and GCE. At sweep rate $> 400 \text{ mV s}^{-1}$, peak I_a merged with the background on using GCE even at pH 7.0 and hence accurate determinations of peak potentials were not possible at GCE. The plot of $\Delta E_{p/2} / \Delta \log v$ versus $\log v$ at pH 7.0 was S-shaped at PGE and indicated the nature of the electrode reaction as EC, in which charge transfer is followed by irreversible chemical reactions.^{13,14}

As uric acid was found as an intermediate during the electrochemical oxidation of xanthine,¹⁵ it was considered interesting to check the formation of 3,7-dimethyluric acid during the oxidation of compound **I**. For this purpose, cyclic voltammograms of 3,7-dimethyluric acid in the pH range 2.2–10.7 were recorded. A well-defined oxidation peak was observed at the same potential, a similar $dE_p/d\text{pH}$ value as noticed for peak II_a in the case of 3,7-dimethylxanthine. Hence, it was concluded that peak II_a corresponds to the oxidation of 3,7-dimethyluric acid, generated by the reduction of peak III_c species.

Controlled potential electrolysis at peak I_a potential of 3,7-dimethylxanthine exhibited a decrease in i_p for peak I_a , exponentially with time. The $\log i_p = f(t)$ plot was a straight line for the first 8–10 min of electrolysis, whereafter a large deviation from the straight line was observed. The deviation from the straight line clearly indicated that the electrode reaction followed a simple path only for the first 8–10 min, of electrolysis and then the followup competitive chemical reactions played a significant role.^{16,17} The experimental values of n for the dimethylxanthine were found to be 4.0 ± 0.2 in the entire pH range studied at both electrodes.

UV-Spectral Studies

The UV spectra of 3,7-dimethylxanthine were recorded in the region 200–350 nm at pH 3.0, 5.0, 7.0 and 8.9 to detect the UV absorbing intermediate generated during the reaction. In the entire pH range, two λ_{max} at around 272 and 207 nm were observed in the UV spectrum of compound **I**. The spectral changes observed at pH 5.0 are presented in Figure 5. Thus, the UV spectrum of 3,7-dimethylxanthine at pH 5.0, exhibited two well-defined bands with λ_{max} 207 and 272 nm and a shoulder at 230 nm (Figure 5 curve 1). Upon application of peak I_a potential, the absorbance at 272 nm systematically decreased whereas an increase in the absorbance in the

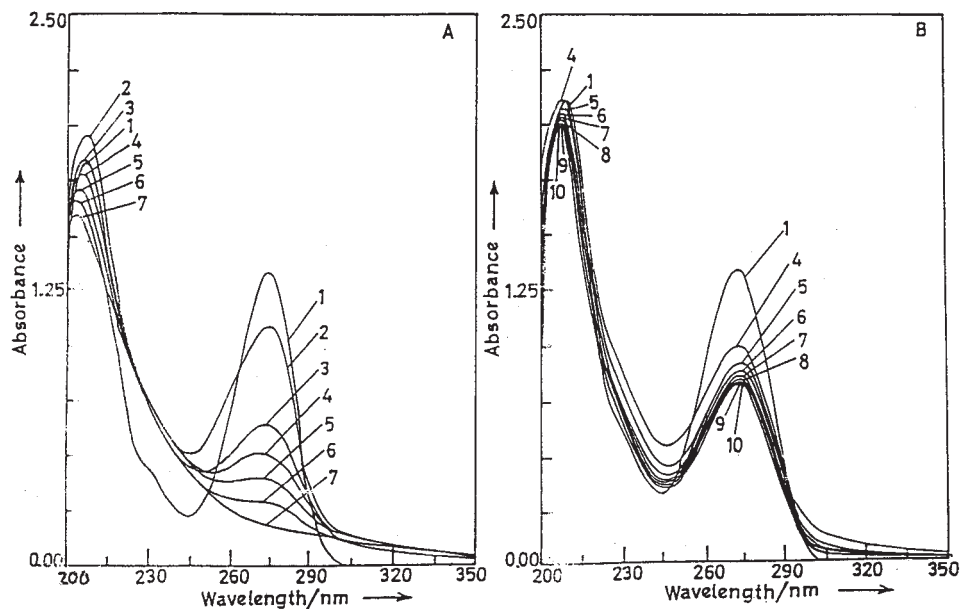


Figure 5. A) Spectral changes observed during electrooxidation of 0.1 mM 3,7-dimethylxanthine at pH 5.0, Pot. 1.5 V *vs.* SCE. Curves were recorded at intervals of 5 min. B) Spectral changes observed after turning off the potential after recording curve (4) in Figure 5A. Curves were recorded at 5 min. intervals.

longer wavelength region 300–350 nm was observed. The absorbance in the 225–260 nm region as well as in the shorter wavelength region (207 nm) increased for the first 5 min (curve 2) and then systematically decreased (curves 3 to 7). If potential was turned off after recording curve 4 in Figure 5A, a systematic decrease in absorbance in the region 215 to 320 nm was observed (Figure 5B).

The kinetic study of the decomposition of the UV-absorbing intermediate was performed at selected wavelengths. For this purpose, the electrolysis was terminated when absorbance at λ_{\max} reached $\sim 50\%$. The absorbance of the intermediate species was monitored at 260, 290 and 320 nm as a function of time and the resulting curves were exponential in nature (Figure 6). The plots of $\log (A-A_{\infty})$ versus time were linear at all pH values and hence suggested that the decomposition reaction of the UV-absorbing intermediate followed first order kinetics. The values of k calculated from $\log (A-A_{\infty})$ versus time plots at different pH are summarized in Table I.

Since cyclic voltammetric studies indicated that peak II_a is due to the formation of 3,7-dimethyluric acid, spectral changes were also monitored for

TABLE I
 Comparison of observed first order rate constant
 for decomposition of the UV intermediate for xanthine
 and 3,7-dimethylxanthine

| pH | λ / nm | $k \cdot 10^3 / \text{s}^{-1}$ |
|----------------------|----------------|--------------------------------|
| 3,7-Dimethylxanthine | | |
| 3.0 | 245 | 1.2 |
| | 272 | 1.2 |
| | 320 | 1.4 |
| 5.0 | 245 | 1.0 |
| | 272 | 1.3 |
| | 320 | 1.0 |
| 7.0 | 245 | 1.3 |
| | 272 | 1.5 |
| | 320 | 1.8 |
| Xanthine | | |
| 3.0 | 225 | 0.9 |
| | 320 | – |
| 5.0 | 225 | 1.8 |
| | 320 | 1.3 |
| 7.0 | 225 | 1.3 |
| | 320 | 1.6 |

3,7-dimethyluric acid (Figure 7). At pH 5.0, dimethyluric acid exhibited three λ_{max} at 290, 237 and 208 nm. Upon application of the potential corresponding to peak II_a, the absorption at λ_{max} systematically decreased whereas absorbance in the region 216–225 nm showed no systematic pattern. An increase of absorbance in the longer wavelength region (300–350 nm) was also noticed. If potential at any stage of oxidation was turned to zero volt, a systematic decrease in the absorbance in the 260–295 and 310–330 nm regions was observed. A plot of absorbance *vs.* time observed at pH 5.0 and at $\lambda = 290$ nm is presented in Figure 6A. The values of the pseudo first order rate constants (k) were calculated at 260, 290 and 320 nm and were found in the range $1.5 - 2.0 \times 10^{-3} \text{ s}^{-1}$. It was interesting to note that the values of k for 3,7-dimethylxanthine and 3,7-dimethyluric acid were essentially similar and hence further augmented our conclusion that the same UV – absorbing intermediate species was generated in both cases. The UV-spectral changes

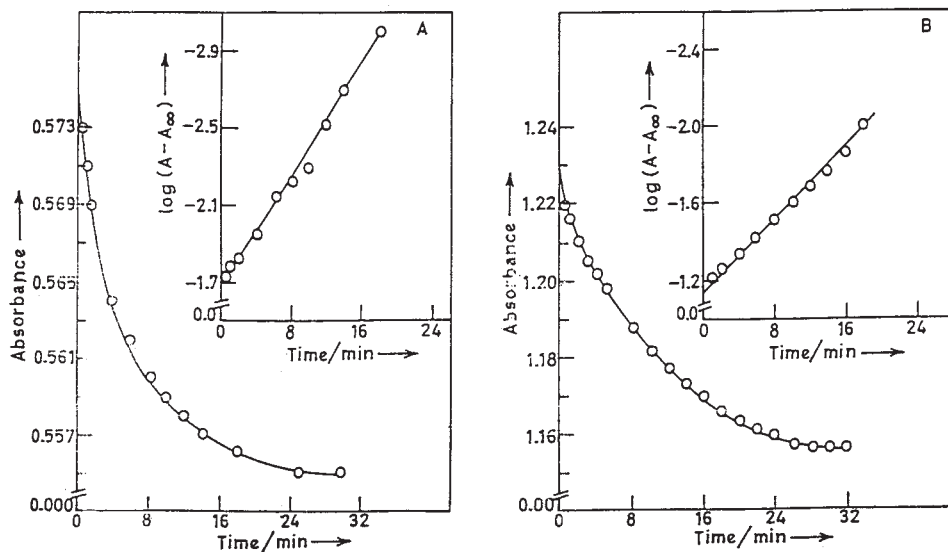


Figure 6. Observed changes in absorbance with time and plot of $\log(A - A_{\infty})$ versus time at pH 5.0 for the UV-absorbing intermediate generated at 290 nm for (A) 3,7-dimethyluric acid (B) 3,7-dimethylxanthine.

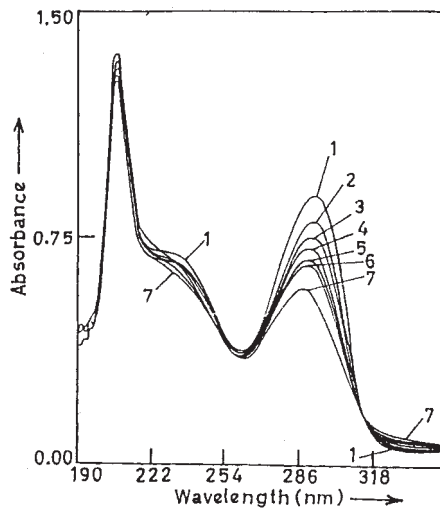


Figure 7. Observed spectral changes during electrooxidation of 3,7-dimethyluric acid at pH 5.0, Pot. 800 mV vs. SCE.

observed for 3,7-dimethylxanthine at pH 3.0 and 8.9 were basically similar to pH 5.0.

Product Isolation and Characterization

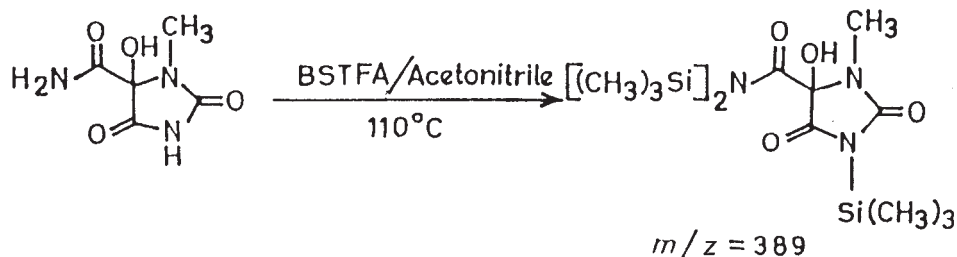
The products of electrooxidation of 3,7-dimethylxanthine were characterized at pH 3.0 and 7.0 at pyrolytic graphite and glassy carbon electrodes. The exhaustively electrolyzed solution was lyophilized and the products were separated by gel permeation chromatography (see experimental). In gel permeation chromatography, at pH 3.0, three peaks, P₁, P₂ and P₃, were observed. Peak P₁ (150–180 mL) and P₂ (180–200 mL) were found to contain buffer constituents (particularly phosphate) and were therefore discarded.

The volume under peak P₃ (225–275 mL) was collected and freeze-dried. The colourless material obtained exhibited a single spot in TLC ($R_f \sim 0.40$) with m.p. 151 °C. The mass spectrum of the material gave a clear molecular ion peak at m/z 174 and thus the molar mass of the material was found as 174. The other high mass peaks observed in the fragmentation were at 137 (5.4%), 136 (2.9%), 129 (5.8%), 128 (94.7%), 109 (19%) and 100 (52.7%). The IR spectrum of the product exhibited prominent bands at 3837, 3785, 3700, 2472, 2319, 1719, 1677, 1434, 1122, 939 and 861 cm^{-1} and the IR spectrum was superimposable by the IR spectrum obtained for the authentic 1-methylalloxan. This product was further confirmed as 1-methylalloxan by recording its ¹H NMR, in which the following signals were obtained – δ/ppm : 2.82 (s, 1H, N–H); 8.20 (s, 3H, C–H) and 8.42 (s, 2H).

The formation of 1-methylalloxan suggests that the imidazole ring breaks and the other products of electrooxidation should be *N*-methylurea. However, *N*-methylurea could not be identified in the present studies. Due to its low molecular weight, it was found to elute between volume 160–180 mL under identical conditions and hence must have been eluted with phosphate, as reported in the case of uric acid and other purines.¹⁸

At pH 7.0, the chromatographic peak P₁ corresponded to phosphate. The colourless lyophilized material obtained under peak P₄ exhibited a single spot in TLC ($R_f \sim 0.36$). It did not give a clear molecular ion peak in the mass spectrum. Hence, it was converted to its trimethylsilyl derivative to make it volatile. GC-MS of the derivatized product exhibited a clear peak with R_t ca. 25.1 min. having a molar mass of 389 (7.2%). The other high mass peaks observed in the fragmentation were at 374 (30.2%), 299 (5.0%), 273 (4.1%), 272 (10.6%) and 262 (2.6%). The molar mass of 389 suggests the product to be 5-hydroxy-1-methylhydantoin-5-carboxamide having three silyl groups. The formation of 5-hydroxyhydantoin-5-carboxamide has been reported during electrooxidation of uric acid.¹⁹ Hence, it is not unusual to get 5-hydroxy-1-methylhydantoin-5-carboxamide during oxidation of 3,7-dimethylxanthine. However, it was found that due to steric hindrance, the H atom of OH group present between C=O and N–CH₃ groups does not undergo silylation. Thus, at pH 7.0 the pyrimidine ring of 3,7-dimethylxanthine opens

to give the ultimate products. The rupture of pyrimidine ring of purines in neutral and alkaline media during chemical oxidation has been well documented in the literature.²⁰

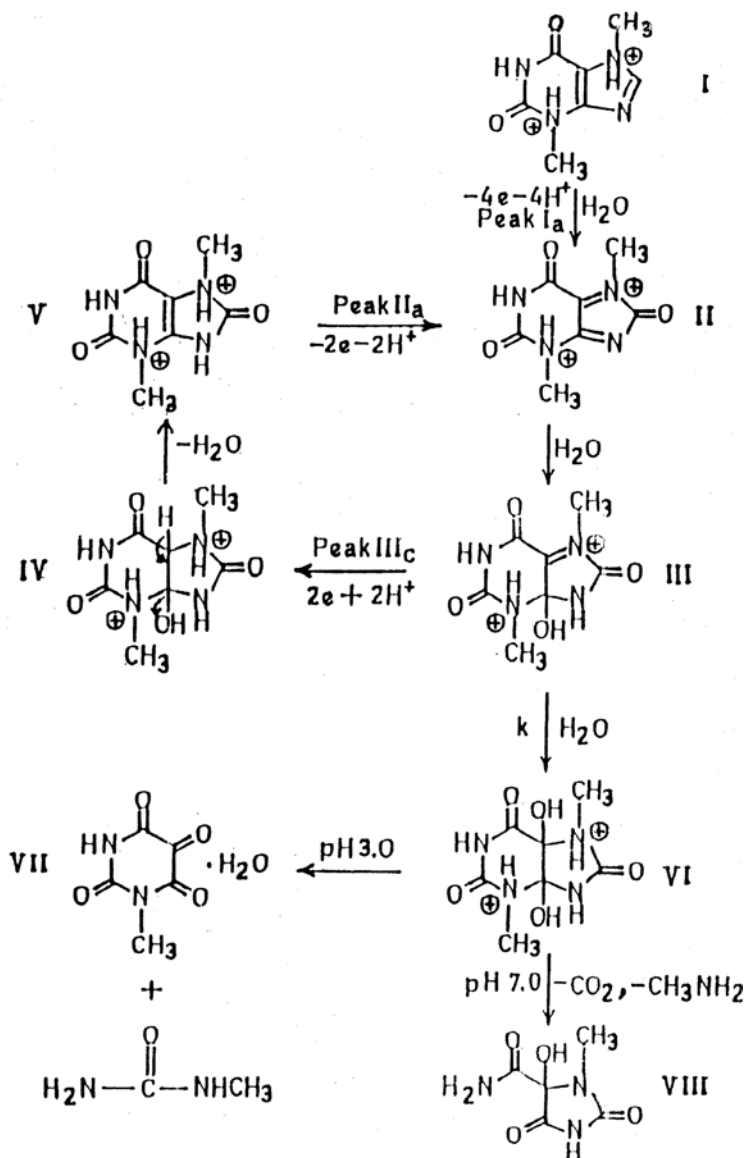


Hence, it is concluded that the products of oxidation of 3,7-dimethylxanthine are 1-methylalloxan and *N*-methylurea at pH 3.0 and 5-hydroxy-1-methylhydantoin-5-carboxamide at pH 7.0. The same products were obtained at the glassy carbon electrode.

The results presented above clearly indicate that the electrooxidation of 3,7-dimethylxanthine proceeds in a single $4e^-$, $4H^+$ pH dependent step to give the corresponding diimine **II**, as shown in Scheme 1. Peak I_a thus represents conversion of compound **I** to **II**. The diimines obtained during the oxidation of purines have been found unstable due to two C=N bonds and are readily attacked by water to give imine alcohol.²¹ The half-life of diimine formed in uric acid oxidation has been found to be 20 ms.²² Thus, it is expected that the diimine **II** would also be unstable and readily attacked by the water in a chemical followup step to give imine alcohol **III**. The presence of methyl groups produced a diimine with a positive charge, localized at N_3 and N_7 positions. Hence, the rate of hydration of diimine **II** seems to be greatly accelerated.

This increase in hydration reaction did not permit the reverse peak to appear in cyclic voltammetry even at a sweep rate of 1 V/s.

The reduction of species **III** at C=N in $2e^-$, $2H^+$ step (peak III_c) would give dihydro molecule **IV** which on losing a molecule of water would give 3,7-dimethyluric acid (**V**). It is observed that peak II_a is noticed in the pH range 2.1–6.0 only when the first negative sweep is extended to peak III_c potentials. The product of peak III_c reaction, 3,7-dimethyluric acid, can also undergo oxidation at PGE to give diimine **II**. The formation of 3,7-dimethyluric acid thus occurs by the reduction of imine alcohol **III** and not by $2e^-$, $2H^+$ oxidation of **I**. Further hydration of imine alcohol species **III** appears to be the step responsible for the decay observed in the first order reaction in the absorbance *vs.* time plot to give diol **VI**.



Scheme 1. A tentative mechanism proposed for the electrooxidation of 3,7-dimethylxanthine at solid electrodes.

At pH 3.0, the imidazole ring opens to give 1-methylalloxan (VII) and *N*-methylurea, whereas at pH 7.0, the pyrimidine ring breaks and decarboxylation gives 5-hydroxy-1-methylhydantoin-5-carboxamide. The rupture of imidazole ring of purines in acidic medium and of pyrimidine ring in neu-

TABLE II

Comparison of peak potentials (E_p) of oxidation peak I_a of xanthines at pH 7.0 and sweep rate 20 mV s⁻¹

| Compound | E_p / mV |
|----------------------|------------|
| Xanthine | 700 |
| 3-Methylxanthine | 912.5 |
| 7-Methylxanthine | 925 |
| 3,7-Dimethylxanthine | 1300 |

tral and alkaline media during chemical oxidation has been extensively reported in literature.^{23,24}

A comparison of the electrochemical behaviour of 3,7-dimethylxanthine with xanthine was also made to determine the effect of methylation on xanthine oxidation. It was found that the peak potential of xanthine (0.70 V at pH 7.0) shifted to a more positive potential in the presence of methyl groups. The extent of the shift towards positive potential at pH 7.0 was close to 600 mV. One of the possible reasons for the shift is the protonation of methyl groups with $pK_a > 11.0$.¹⁰ The positive charge thus produced in pyrimidine as well as imidazole rings makes the removal of electrons difficult. A comparison of E_p of xanthine, 3-methylxanthine, 7-methylxanthine and 3,7-dimethylxanthine at pH 7.0 is presented in Table II. It was clearly noticed that the shift in E_p for 3- or 7-methylxanthine from xanthine is ~ 200 mV. Thus, the shift expected for 3,7-dimethylxanthine is 400 mV. However, the experimental values of E_p observed for 3,7-dimethylxanthine indicated a shift of 600 mV. Thus, the substituent effect is not additive and one of the possible reasons for such non-additivity is the distortion in the planar nature of the molecule, which may restrict the proper orientation of the molecule at the electrode surface before the electron transfer can take place.

The rate of decay of the UV absorbing intermediate in xanthine and 3,7-dimethylxanthine did not show much difference and the values were 1.3×10^{-3} and 1.7×10^{-3} s⁻¹, respectively. It was interesting to observe that, at pH 3.0, oxidation of 3,7-dimethylxanthine gave products similar to xanthine and that the products were appropriately methylated. On the other hand, at pH 7.0, oxidation of xanthine gives allantoin as the major product along with 5-hydroxyhydantoin-5-carboxamide. In dimethylxanthine, no formation of allantoin was observed and 5-hydroxy-1-methylhydantoin-5-carboxamide was obtained as the major product. This difference in behaviour can be accounted for by the presence of methyl groups at positions 3 and 7, which limit the number of possible resonating structures and produce steric

effects. The presence of methyl groups at positions 3 and 7 does not permit the ring contraction either due to the presence of positive charge in the pyrimidine ring and imidazole ring, which is the primary requirement for the formation of allantoin.²⁵ Thus, the presence of methyl groups at positions 3 and 7 in xanthine makes the oxidation difficult and alters the redox behaviour by its electron donating nature. At this stage it is not possible to correlate the central behavioural stimulant activity with the observed oxidation behaviour. However, it is possible that various species generated in the redox mechanism (Scheme 1) may act as competitive antagonists to adenosine at A₁ and A₂ receptors due to their structural similarities.

Acknowledgement. – One of the authors (AR) is thankful to the CSIR, New Delhi, for providing financial assistance for this work in the form of a Senior Research Fellowship.

REFERENCES

1. K. A. Jacobson, L. Kiriasis, S. Brona, B. J. Bradbury, U. Kamanula, J. M. Campagna, S. Secunda, J. W. Daly, J. L. Neumeyer, and L. W. Pfleiderer, *J. Med. Chem.* **32** (1989) 1873–1879.
2. S. H. Snyder, J. J. Katims, Z. Annau, R. F. Bruns, and J. W. Daly, *Proc. Natl. Acad. Sci. USA*, **78** (1981) 3260–3268.
3. R. I. Ogilvie, in: *Anti-Asthma Xanthines and Adenosine*, K.-E. Andersson and G. A. Persson, (Eds.), Excerpta Medica, Amsterdam, 1985, p. 327.
4. N. Svedmyr, in: *Anti-Asthma Xanthines and Adenosine*, K.-E. Andersson and G. A. Persson, (Eds.), Excerpta Medica, Amsterdam, 1985, p. 135.
5. S. R. R. Musk and G. G. Steel, *Int. J. Radiat. Biol.* **57** (1990) 1105.
6. G. D. Christian and W. C. Purdy, *J. Electroanal. Chem.* **3** (1962) 363–373.
7. R. N. Goyal, S. K. Srivastava, and R. Agarwal, *Bull. Soc. Chim. Fr.* (1985) 656–659.
8. H. K. Chan and A. G. Fogg, *Anal. Chem. Acta* **105** (1979) 423–428.
9. J. J. Lingane, *Electroanalytical Chemistry*, 2nd ed., Wiley Interscience, 1966, p. 222.
10. D. D. Perrin, B. Dempsey, and E. P. Serjeant, *pK_a Prediction for Organic Acids and Bases*, Chapman and Hall, London, 1981, p. 19.
11. R. S. Nicholson and I. Shain, *Anal. Chem.* **36** (1964) 706–723.
12. R. H. Wopschall and I. Shain, *Anal. Chem.* **39** (1967) 1514–1527.
13. P. H. Reiger, *Electrochemistry*, Prentice Hall, New Jersey, 1987, p. 343.
14. E. C. Brown and R. F. Large, in: *Techniques of Chemistry*, A. Weissberger and R. W. Rossiter, (Eds.) Wiley-Interscience, New York, 1974, p. 423.
15. R. N. Goyal, *Indian J. Chem. Sect. A*, **28A** (1989) 467–471.
16. G. Cauquis and V. D. Parker, in: *Organic Electrochemistry*, M. M. Baizer (Ed.), Marcel Dekker, New York, 1973, p. 134.
17. L. Meites, in: *Physical Methods of Chemistry*, A. Weissberger and R. W. Rossiter, (Eds.), Wiley, New York, 1974, p. 134.

18. R. N. Goyal, A. K. Srivastava, and V. Bansal, *J. Chem. Soc., Perkin Trans. 2* (1994) 1709–1715.
19. R. N. Goyal, A. B. Toth, and G. Dryhurst, *J. Electroanal. Chem.* **131** (1982) 181–202.
20. V. H. Brederick, F. Effenburger, and G. Rainer, *Ann. N. Y. Acad. Sci.* **82** (1964) 673.
21. G. Dryhurst, K. M. Kadish, F. Scheller, and R. Renneberg, *Biological Electrochemistry*, Vol. 1. Academic press, 1982, p. 279.
22. H. A. Marsh and G. Dryhurst, *J. Electroanal. Chem.* **95** (1979) 81–97.
23. A. Albert and D. J. Brown, *J. Chem. Soc.* (1954) 2060–2071.
24. E. Shaw, *J. Org. Chem.* **27** (1962) 883–885.
25. R. N. Goyal, V. Bansal, and M. S. Verma, *Bull. Soc. Chim. Fr.* **130** (1993) 146–153.

SAŽETAK

Kemija oksidacije 3,7-dimetilksantina

Rajendra N. Goyal i Arshi Rastogi

Proučavana je elektrokemijska oksidacija 3,7-dimetilksantina u području $2,1 < \text{pH} < 10,7$, i to na pirolitičkom grafitu, platini i staklastim ugljikovim elektrodama. Elektrooksidacija 3,7-dimetilksantina na krutim elektrodama odvijala se u jednom pH-ovisnom koraku, dajući diimine koji su se raspadali u nekoliko koraka. Intermedijar koji je apsorbirao UV i koji je nastajao za vrijeme elektrooksidacije 3,7-dimetilksantina, raspadao se približno istom brzinom kao 3,7-dimetilksantin, slijedeći kinetiku prvoga reda. Karakterizirani su produkti elektrooksidacije 3,7-dimetilksantina, te je predložena reakcijska shema njihova nastajanja. Razmotren je također utjecaj metilnih skupina na elektrooksidaciju ksantina.